

Supporting Online Material for

Synapse- and Stimulus-Specific Local Translation During Long-Term Neuronal Plasticity

Dan Ohtan Wang, Sang Mok Kim, Yali Zhao, Hongik Hwang,
Satoru K. Miura, Wayne S. Sossin, Kelsey C. Martin*

*To whom correspondence should be addressed. E-mail: kcmartin@mednet.ucla.edu

Published 14 May 2009 on *Science Express*
DOI: 10.1126/science.1173205

This PDF file includes:

Materials and Methods
Figs. S1 to S17
References

Synapse- and Stimulus-Specific Local Translation During Long-Term Neuronal Plasticity

Supporting Online Material

Materials and Methods

Reporter Constructs:

pDendra2-N (Evrogen, Moscow, Russia) coding sequence (including stop codon) was PCR-amplified and cloned into pNEX3 as a XbaI/BamHI fragment (pNEX-Dendra). The 3'UTR of sensorin was cloned from an *Aplysia* sensory neuron process library (S1) and PCR-amplified as a BamHI/BamHI fragment. The 5'UTR was obtained from an *Aplysia* 5'RACE cDNA library and PCR-amplified as a SalI/SalI fragment (see fig S1 for sensorin 5'UTR, 3'UTR sequences, and for maps of constructs). The two UTR fragments were then independently inserted into pNEX3-Dendra to generate chimeric reporters: pNEX3-Dendra-3'UTR, and pNEX3-5'UTR-dendra-3'UTR. mCherry and VAMP coding sequences were PCR-amplified and independently subcloned into pNEX3 (XbaI/SmaI) to generate a single reading frame as pNEX3-VAMP-mCherry.

***Aplysia* cell culture, microinjection, electrophysiology, stimulation and pharmacological treatments:**

A detailed protocol for *Aplysia* SN-MN culture preparation can be found at <http://www.biolchem.ucla.edu/labs/martinlab/>. SN and LFS MNs were obtained from 80—100 gram *Aplysia* (Alacrity, Redondo Beach, CA). L11 motor neurons were microdissected from the abdominal ganglion of juvenile *Aplysia* (1-4 g, National *Aplysia* Resource, University of Miami, FL). During culturing, the MN and SN cell bodies were carefully positioned so that the MN would not suffer any mechanical damage when SN cell body was removed during the experimental protocol. Reporter plasmids were microinjected into SNs 24-36 hrs after plating. 48hrs later, reporter expression was monitored in the SNs by fluorescence microscopy, and the cell bodies of dendra-expressing SNs were removed along with ~50 microns of proximal axon segment with a sharp electrode as described in (S2). Cultures were excluded from further experiments if any visible damage to MN occurred during cell body removal process. Synaptic connectivity was assessed by measuring EPSP amplitude between SN and target MN. SN and MN were impaled

with sharp glass electrodes (20–40 mΩ resistance) filled with 1.5 M K-acetate, 0.5 M KCl, and 0.01 M HEPES (pH 7.2). MNs were held at -80 mV, and SNs were held at -50mV. EPSPs were evoked by intracellular stimulation of the sensory neuron (1–3 nA for 5 ms) with a Grass (West Warwick, RI) S88 stimulator. EPSPs were recorded and measured with Axoscope 8.2 and pCLAMP 8 software (Axon Instruments, Union City, CA). To elicit cell-wide long-term facilitation (LTF) of SN-MN synapses, cultures received five spaced applications of 5HT according the following protocol: five 5 min applications of 5HT (10 µM) with four intervening 20 min washes of 50%L15/50%ASW, with a total stimulation time of 1hr 45 min. To induce synapse-specific LTF and LTD, we locally perfused 5HT or FMRFamide as described in Martin, 1997 and Guan, 2001, respectively(S2, S3). Briefly, 100µM 5HT or 10µM FMRFamide in 50% L15/50% ASW containing 0.2% fast green was applied to a subset of synapses using a perfusion electrode (approximately 1MΩ resistance). The electrode was connected to a picospritzer (World Precision Instruments, Sarasota, FL) and very low pressure (approximately 1psi) was used to apply five 5s pulses of drugs at 10s interval as one stimulation (fig. S3). Air pressure and bulk flow in the bath (approximately 1ml/min) were adjusted so that most of synapses in a 63X objective field were locally perfused, without any perfusion of synapses in other fields. The stimulation was repeated five times, with four intervening 10 min bath perfusions of 50% L15/50% ASW, for a total stimulation time of 50 min. Anisomycin (10µM; Calbiochem, San Diego, CA) was present for 30 min before and during stimulation. 5HT-creatine was from Sigma (Saint Louis, MO) and FMRFamide was from Calbiochem (San Diego, CA). L15 was purchased from Sigma (Saint Louis, MO), and ASW consisted of NaCl 27.89g, CaCl₂•2H₂O 1.62g, KCl 0.738g, MgCl₂•6H₂O 11.18g, HEPES 2.38g in 1L nanopure water. All solutions were filtered through 0.2µm filters before use. BAPTA tetraacetic acid was purchased from Sigma (San Louis, MO) and dissolved in 1.5M K-acetate, 0.5M KCl, 0.01M HEPES (pH 7.2) at injecting concentration of 50mM.

Live cell imaging and image analysis:

All confocal images were taken on Zeiss Pascal scanning laser microscope (Zeiss, Germany). We began image acquisition 18 hrs after removal of the SN cell body to allow recovery time from

injury. To photoconvert dendra2, samples were illuminated with UV light from a 100 W Hg lamp (using a 409 nm filter) for approximately 2" at 100% power using a 63X oil Apochromat objective. Native, unphotoconverted (green) dendra2 protein was excited with a 488nm Argon laser at 2.5mW and collected through BP 505-600 filter. Fluorescence signals from photoconverted dendra2 was excited with a 543nm He-Ne laser at 0.8mW and collected through BP560-615 filter; the pinhole was set at 1 airy unit for images acquired both at 10X and 63X magnification, with slice intervals of 6.4 μ m and 0.8 μ m, respectively. VAMP-mCherry was excited with a 543nm He-Ne laser and collected through LP560 filter, and Alexa Fluor 647 was excited with a 633nm He-Ne laser and collected through LP650 filter. Two-dimensional projections of an equal number of slices were made, using maximum mode to allow pixel intensities along the same Z-axis to collapse into one illuminated image. The red fluorescence signal from photoconverted dendra2 served as an important control to monitor i) the original expression level of dendra2; ii) cell integrity (e.g. dramatic decreases in red fluorescence indicates leakiness of the plasma membrane); and iii) morphological changes that occurred over the course of imaging. The growth of new synaptic connections induced by this stimulation protocol does not occur until 12-18 hrs following 5HT application (S4, S5). Cells in which there was greater than a 20% decrease in red fluorescence were excluded from analysis; the mean ratio (as F_{end}/F_{start}) in red fluorescence across all experiments was 1.0 ± 0.003 . To optimize neuronal health and protect neurons from phototoxicity during photoconversion and imaging, Trolox (Tokyo Chemical Industry, Japan), a Vitamin E derivative, was included in the media.

To measure new translation, total fluorescence (area (μm^2) X MEAN fluorescence intensity) of both green and red fluorescence as well as the total RNA intensity of each synaptic site that had reporter mRNA cluster, were measured by a "blind" observer using LSM software. New translation was estimated as the total pixel intensity in the green channel after stimulation minus the total intensity in the green channel before stimulation, divided by the total intensity in the green channel before stimulation, $(F_{end}-F_{start})/F_{start}$, or $\Delta F/F$. To correct for volume changes, F_{end}/F_{start} for the green signal was normalized to F_{end}/F_{start} for red signal. To quantify the difference between new translation at stimulated (perfused) and unstimulated (non-perfused) synapses

within a single neuron, we acquired images at 3-4 non-perfused sites, which were chosen on the basis of their morphological similarity to the perfused site. We quantified new translation at each synaptic site within a field (perfused or non-perfused) and calculated the mean new translation ($\Delta F/F$). The difference was then quantified as the ratio of mean new translation at perfused sites to mean new translation at multiple non-perfused sites. Note that the mean new translation at the 3-4 non-perfused fields per neuron was averaged to generate the mean $\Delta F/F$ for non-perfused sites. To validate this approach, we compared the mean new translation between two non-perfused sites within the same neuron, and found that the ratio was 1.0.

Fluorescence in situ hybridization (FISH):

Immediately after live cell imaging, cells were fixed with 4%PFA/30% sucrose in PBS and processed for FISH. The dendra2 coding sequence was amplified and cloned into pCR4. Antisense riboprobes (750 bp) were generated by *in vitro* transcription from the T7 promoter (Roche, Indianapolis, IN). In control experiments, the sense riboprobe did not produce any higher background signal than uninjected cells. The integrity of the riboprobes was tested by agarose gel electrophoresis and the efficiency of DIG incorporation was estimated by dot blotting on nylon membranes and comparing to standard RNA probes (Roche, Indianapolis, IN). FISH detection using the TSA amplification system was done exactly as previously described by Lyles et al, 2006 (S6), with hybridization at 58°C. Since dendra2 protein fluorescence does not persist following processing of samples for FISH, we manually aligned RNA images to live cell images based on the morphology of SN and MN. To simultaneously detect reporter mRNA and endogenous sensorin in SNs, we made DIG labeled dendra2 riboprobes and Biotin labeled reporter mRNA riboprobes (and vice versa). Sensorin riboprobes were made as described in Lyles et al., 2006 (S6). Both riboprobes were included in one hybridization step. The FISH detection protocol was modified so that anti-DIG-peroxidase and anti-Biotin-peroxidase antibody detections were carried out sequentially with a H₂O₂ incubation step added in between to quench the peroxidase activity of the first antibody.

Statistical analysis:

All results were collected from at least three independent experiments. Prism Graphpad software (La Jolla, CA) was used for all statistical analysis. Paired and unpaired Students' t-tests were performed when data distribution passed normality tests, otherwise Wilcoxon-Mann-Whitney nonparametric tests were used. When three or more groups were compared, data were analyzed by One-Way ANOVA and Bonferroni's multicomparison tests.

Supporting figure legends

Fig. S1: Sequences of 5' and 3' UTRs of sensorin; maps of translational reporter constructs. Shown are cartoons of the constructs used in the study, containing the control UTRs from SV40, 5', 3' or 5' and 3' UTRs of sensorin. Constructs were made in pNEXδ3 vector (S7). Also shown are the 5' and 3' UTR sequences of sensorin.

Fig. S2: The 3'UTR of sensorin targets reporter mRNA to neuronal processes but does not promote concentration at synapses. **(A)** Colocalization of 3'UTR sensorin reporter mRNA and endogenous sensorin mRNA. Expression vectors encoding the sensorin (3'UTR) translational reporter were microinjected into *Aplysia* sensory neurons (SNs, isolated, or co-cultured with motor neurons, MNs) on DIV2. Cultures were fixed 48 hrs later and processed for double label FISH using DIG-labeled dendra2 riboprobes and biotin-labeled sensorin probes. Representative confocal images of DIC/merged (**A1, 2**), dendra2 reporter mRNA in red (**A3, 5**) and endogenous sensorin mRNA in green (**A4, 6**). FISH signals are shown in isolated SNs (**A1, 3, 4**) and in SNs paired with MNs (**A2, 5, 6**). Arrows point to areas where only endogenous sensorin mRNA was observed. Note that the 3'UTR is sufficient to transport the reporter RNA to distal neurites (**A3**). Scale bar: 50μm. Colocalization was quantified as colocalization coefficient (0, no colocalization; 1, perfect colocalization); **(B)** VAMP-mCherry and reporter were co-expressed in SN, and the MN was labeled with Alexa 647. Synapses were detected as VAMP-mCherry varicosities contacting the MN. **B1:** Low magnification images of reporter protein (green), VAMP-mCherry (red) and MN (blue) with boxes of higher magnification images in **a1** and **b1**. Cells were fixed after imaging and processed for FISH for reporter mRNA in **B2, a2** and **b2**. Scale bar: 50μm. **(C)** Quantification of

percent of sites that contained VAMP-mCherry and/or reporter mRNA.

Fig. S3: Top cartoon illustrates experimental strategy for using dendra2-based translational reporters. Confocal images in bottom panel show cultured SN-MN with SN expressing dendra2 reporter (left), SN soma removal (middle), and photoconversion of dendra2 throughout the entire neuronal arbor before treatment (right). Scale bar: 50 μ m.

Fig. S4: Control experiments for fig 2: representative images of reporter translation in 5XASW vehicle control, untreated control, and cultures treated with 5XASW and 5X5HT in the presence of the protein synthesis inhibitor anisomycin. **(A1)** Low magnification image of a SN expressing the dendra2-reporter in a SN-MN coculture. The dashed circle outlines the location of the removed soma. **(A2 and A3)** High magnification DIC/merged image of area outlined by the red box in **A1**, showing synaptic contacts between SN and MN before (**A2**) and after (**A3**) UV photoconversion. **(A4 and A5)** Green dendra2 signal remaining following photoconversion, before (**A4**) and after (**A5**) vehicle stimulation (5XASW). Lack of green dendra2 indicates efficient photoconversion, new green dendra2 reveals modest new translation post 5xASW. **(A6 and A7)** Photoconverted red dendra2 signal before (**A6**) and after (**A7**) 5xASW shows SN volume. **(A8)** Cells were fixed at the end of the experiment and processed for FISH with antisense dendra2 riboprobes. **(B1-7)** 5XASW treatment in the presence of anisomycin (10 μ M). **(C1-7)** Control images taken from untreated cultures. **(D1-7)** 5X5HT treatment in the presence of anisomycin (10 μ M). Modest increases in green dendra signal were detected following 5xASW (**A4-5**) and in untreated control cultures, reflecting basal translation; no increase in green dendra signal was observed in the presence of anisomycin (**B4, 5** and **D4, 5**), demonstrating that the new green signal resulted from new translation. **(A8, B8, C8, D8)** RNA staining at the end of experiments reveals equivalent RNA intensity across experiments. Scale bar: 50 μ m.

Fig. S5: Photomicrograph illustrating local perfusion. Neurites of a SN expressing the green

dendra reporter (the SN cell soma has been removed), in contact with an LFS MN. A perfusion electrode (dotted line) was used to locally deliver stimuli (5XASW, 1X5HT, 5x5HT, or 5XFMRFa) to a subset of synapses, with bulk flow (blue triangle) in the bath directing the flow away from the rest of the neuronal arbor. Fast green dye was included to visualize the perfused area (green-blue stream). Scale bar: 50 μ m.

Fig. S6: Pre-photoconversion images and photoconverted (red) dendra images to accompany fig 3. (A-C panels 1 and 2) Merged DIC, green and red images of boxed regions (from fig. 3) showing sites of synaptic contact before UV photoconversion. **(A-C panels 3-6)** Confocal images of red dendra signal after photoconversion and before (pre) and after (post) local perfusion. Note that no significant morphological changes occurred during the stimulation, as indicated by the lack of change in the red dendra signal. Scale bar: 50 μ m.

Fig. S7: Local perfusion of 5XASW does not stimulate translation of 5'3'UTR reporter. (A) Low magnification images indicating perfused region (black box), non-perfused region (white box), removed SN soma (dashed circle), and direction of local perfusion (blue arrow). **(Panels A1 and A2)** Merged DIC, green and red images of boxed regions showing sites of synaptic contact before UV photoconversion. **(Panels A3-6)** Pseudocolored confocal images of green dendra2 signal after photoconversion and before (pre) and after (post) local perfusion. **(Panels A7-10)** Confocal images of red dendra2 signal after photoconversion and before (pre) and after (post) local perfusion. **(Panels A11 and A12)** RNA staining at the end of experiments reveals equivalent RNA intensity in both perfused and non-perfused sites. No significant morphological changes occurred during the stimulation, as indicated by the lack of change in the red dendra2 signal. Scale bars: 50 μ m.

Fig. S8: 1X5HT followed by 4XASW, which produces short-term facilitation, does not stimulate translation of the 5'3'UTR reporter. (A) Low magnification images indicating perfused region (black box), non-perfused region (white box), removed SN soma (dashed circle),

and direction of local perfusion (blue arrow). (**Panels A1 and A2**) Merged DIC, green and red images of boxed regions showing sites of synaptic contact before UV photoconversion. (**Panels A3-6**) Pseudocolored confocal images of green dendra2 signal after photoconversion and before (pre) and after (post) local perfusion. (**Panels A7-10**) Confocal images of red dendra2 signal after photoconversion and before (pre) and after (post) local perfusion. (**Panels A11 and A12**) RNA staining at the end of experiments reveals equivalent RNA intensity in both perfused and non-perfused sites. No significant morphological changes occurred during the stimulation, as indicated by the lack of change in the red dendra2 signal. Scale bars: 50 μ m.

Fig. S9: Local perfusion of 5XASW, which does not produce long-term facilitation, does not stimulate translation of the 3'UTR reporter. (**A**) Low magnification images indicating perfused region (black box), non-perfused region (white box), removed SN soma (dashed circle) and direction of local perfusion (blue arrow). (**Panels A1 and A2**) Merged DIC, green and red images of boxed regions showing sites of synaptic contact before UV photoconversion. (**Panels A3-6**) Pseudocolored confocal images of green dendra2 signal after photoconversion and before (pre) and after (post) local perfusion. (**Panels A7-10**) confocal images of red dendra2 signal after photoconversion and before (pre) and after (post) local perfusion. (**Panels A11 and A12**) RNA staining at the end of experiments showed comparable RNA intensity in both perfused and non perfused sites. No significant morphological changes occurred during the stimulation, as indicated by the lack of change in the red dendra2 signal. Scale bars: 50 μ m.

Fig. S10: Quantification of new translation and RNA intensity in local stimulation experiments included in fig 3 and S6-9. New translation was quantified as described in the supporting online methods section, and results were grouped across experiments. The analysis of the differences in figure 3-5 was measured in each neuron (intraneuron comparison) and the results are presented as a ratio between $\Delta F/F$ at perfused and non-perfused sites. Here, we present the group data by showing the mean $\Delta F/F$ at perfused sites and at non-perfused sites (instead of showing them as a ratio of perfused/non-perfused) (**A**) Group analysis accompanying

fig 3. New translation at non-perfused synapses and at synapses perfused wtih 5XASW, 1X5HT, 5X5HT, or 5XFMRFa. There was no significant difference in translation at non-perfused synapses. Only synapses perfused with 5X5HT showed significantly higher translation (** $p<0.001$, Wilcoxon-Mann-Whitney test). **(B)** Analysis of mean RNA intensity for each imaged field showed that there was no significant difference in the concentration of RNA between perfused and non-perfused regions, or between cells treated with different stimuli. Thus, the increase in translation with local application of 5x5HT cannot be attributed to differences in RNA concentrations.

Fig. S11: Pre-photoconversion images and photoconverted (red) dendra images to accompany fig 4. (A-B panels 1 and 2) Merged DIC, green and red images of boxed regions (from fig. 3) showing sites of synaptic contact before UV photoconversion. **(A-B panels 3-6)** Confocal images of red dendra2 signal after photoconversion and before (pre) and after (post) local perfusion. Note that no significant morphological changes occurred during the stimulation, as indicated by the lack of change in the red dendra2 signal. Scale bar: 50 μ m.

Fig. S12: Controls for fig 4: 5XASW did not simulate translation of reporters expressed in either isolated SNs or SNs paired with non-target motor neuron L11. (A and B) Low magnification images indicating perfused region (black box), non-perfused region (white box), removed SN soma (dashed circle) and direction of local perfusion (blue arrow). **(A-B panels 2 and 3)** Merged DIC, green and red images of boxed regions showing sites of synaptic contact before UV photoconversion. **(A-B panels 4-7)** Pseudocolored confocal images of green dendra2 signal after photoconversion and before (pre) and after (post) local perfusion. **(A-B panels 8-11)** Confocal images of red dendra2 signal after photoconversion and before (pre) and after (post) local perfusion. **(A-B panels 12 and 13)** RNA staining at the end of experiments revealed equivalent RNA intensity in both perfused and non-perfused sites Note that no significant morphological changes occurred during the stimulation, as indicated by the lack of change in the red dendra2 signal. Scale bars: 50 μ m.

Fig. S13: Quantification of new translation and RNA intensity in local stimulation experiments included in Fig. 4, S11, and S12. (A) Group data of new translation. (B) RNA staining intensity (Wilcoxon-Mann-Whitney test).

Fig. S14: Acute injection of BAPTA completely blocks depolarization-induced intracellular calcium elevations in MNs but did not affect either endogenous sensorin or reporter mRNA concentration at synapses. (A) SNs were cocultured with LFS MNs. On DIV5, 50mM BAPTA (**A3 and A4**) or vehicle (1.5M K-acetate, 0.5M KCl, 0.01M HEPES (pH 7.2), **A1, A2**) were injected into cytoplasm of LFS motor neurons together with Fluo4 (5 mM). Confocal images were acquired when cultures were in ASW (**A1, A3**) or 100mM KCl (added to the bath to depolarize the cells, **A2, A4**). The increase in Fluo4 signal was quantified as $\Delta F/F \times 100$, %. (B) In parallel experiments, cultures were fixed 1hr after BAPTA/vehicle injection, and processed for FISH to detect endogenous sensorin (green) and reporter mRNA (red) clustering. In control cultures, MNs were injected with vehicle (**B1, B2**); in experimental cultures, MNs were injected with BAPTA (**B3, B4**). BAPTA injection did not alter the concentration of either reporter mRNA (**B2, B4**) or endogenous sensorin mRNA (**B1, B3**) at synapses, as quantified by measuring the coefficient of variation (Lyles et al. 2006 and unpublished data). Scale bars: 50 μ m.

Fig. S15: Pre-photoconversion images and photoconverted (red) dendra images to accompany fig. 5. (A-B panels 1 and 2). Merged DIC, green and red images of boxed regions (from Fig. 5) showing sites of synaptic contact before UV photoconversion. (A-B panels 3-6) Confocal images of red dendra2 signal after photoconversion and before (pre) and after (post) local perfusion. Note that no significant morphological changes occurred during the stimulation, as indicated by the lack of change in the red dendra2 signal. Scale bar: 50 μ m.

Fig. S16: Quantification of new translation and RNA intensity in local stimulation experiments included in fig. 5. (A) Group data from fig. 5, quantifying new translation. (B) Mean

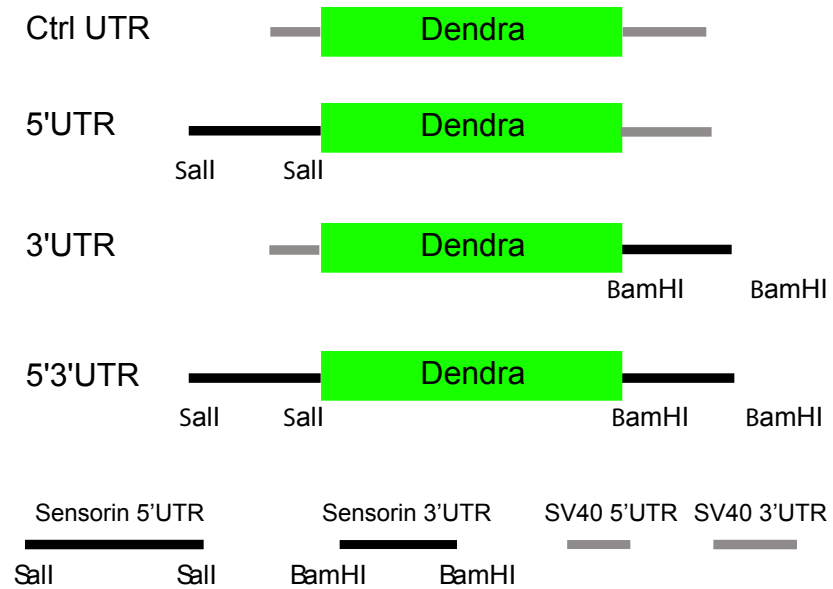
RNA staining intensity at stimulated and unstimulated sites ($*p<0.05$, Wilcoxon-Mann-Whitney test).

Fig. S17: Diffusion of dendra protein at varicosities and neuritic shafts of sensory neurons (SNs). To estimate the diffusion of newly synthesized dendra2, we took advantage of the fact that diffusion of dendra protein can be determined by measuring the kinetics with which locally photoconverted red dendra2 signal is lost from varicosities (A) and/or neuritic shafts (D). (A) Focal UV illumination (2") produced local red dendra2 fluorescence (detected with 543nm illumination). Red dendra2 fluorescence in the varicosity was then monitored by time-lapse confocal microscopy at 10 sec (A1) including 2" photoconversion, switching to scan mode and scanning time, 1 min (A2), 5 min (A3), and 10 min (A4). The red dendra2 fluorescence signal in the varicosity decayed over this time period, accompanied by an increase in green dendra2 fluorescence. (B) The diffusion of the red signal from the site of photoconversion (0") for the experiment in A. (C) The decay of red fluorescence in the varicosity was well fit by a single exponential and plateaued at 10 min, with more than 40% of the initial red fluorescent signal remaining in the varicosity. (D) Diffusion of photoconverted dendra2 in the neuritic shaft was much faster: when we focally photoconverted dendra2 in the shaft, the first image after photoconversion (10") already revealed a diffusion of red fluorescence in the shaft and diffused rapidly, indicating much faster diffusion than varicosities. (E) We measured diffusion in the shaft of fixed SNs (following fixation with 4%PFA/30%sucrose/PBS). These experiments showed no diffusion or obvious photobleaching, which could have contributed to the apparent decay rate. Together, these results indicate that the diffusion of synaptically synthesized dendra2 is likely much slower than the rate of diffusion of dendra2 protein in the neuritic shaft (also see diffusion of PAGFP at spines by Bloodgood BL and Sabatini BL (S8)). This property likely explains why we were able to observe accumulation of newly synthesized reporter at synapses. Note that we also generated reporters in which we added a myristylation signal to dendra2 (using the myristylation signal from PTEN) in order to further limit diffusion of the newly translated reporter, but found that this targeted the reporter to internal membranes and compromised the health of

reporter-expressing SNs.

References

- S1. R. Moccia *et al.*, *J Neurosci* **23**, 9409 (2003).
- S2. K. C. Martin *et al.*, *Cell* **91**, 927 (1997).
- S3. Z. Guan *et al.*, *Cell* **111**, 483 (2002).
- S4. J. H. Kim *et al.*, *Neuron* **40**, 151 (2003).
- S5. H. Udo *et al.*, *Neuron* **45**, 887 (2005).
- S6. V. Lyles, Y. Zhao, K. C. Martin, *Neuron* **49**, 349 (2006).
- S7. B. K. Kaang, *Neurosci Lett* **221**, 29 (1996).
- S8. B. L. Bloodgood, B. L. Sabatini, *Science* **310**, 866 (2005).

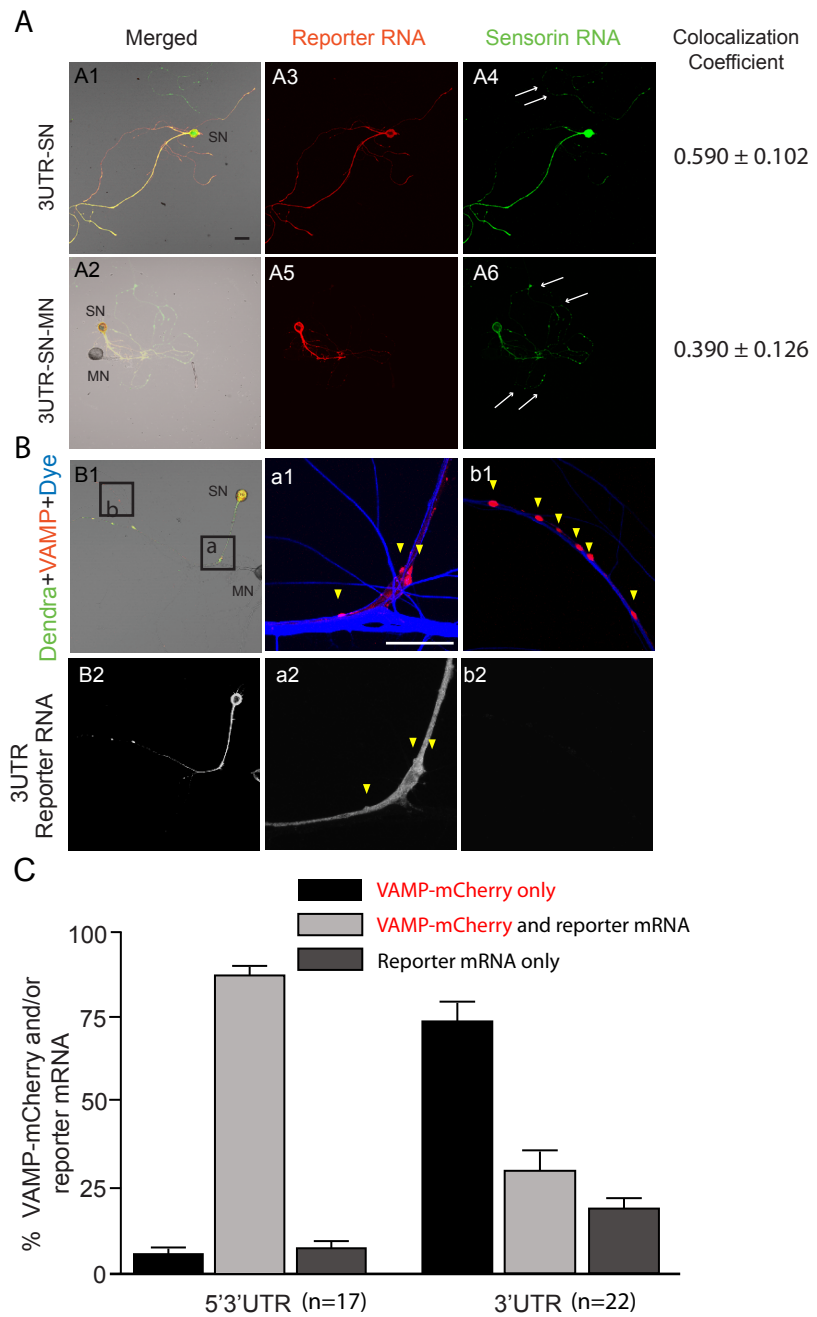


Sensorin 5'UTR

1 CCACTGTGGC GACAGGGCTT GGCACGATAC GACACACTCA CAATTTGCG GGTGAACCAC
 61 GTGGCCCCTT CCTCGCTGAT TTTCACGCTT GCGGATTCTG GCTAAAAGA CAGGGCCAGG
 121 GGTGCACTT TGAGGAAACA CAGGTGCTAA TTTATTGCCG TGTCACCTTT ACGTATAAAA
 181 CGCAGGCCGC TTTGCTCGAA CATTAGAAC AGAGAACTGA GAGCTCAAAG ATACATTCCA
 241 GTCTTGAAAC AGAAACAGTC TTTCCCCGAT CCCAAAAACT AACACAGATA AGTGAGCAAC//

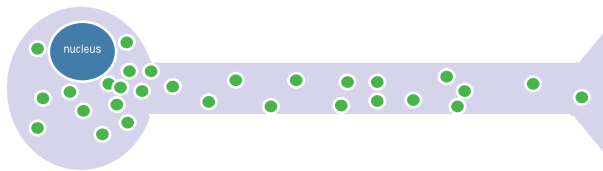
Sensorin 3'UTR

1 CGGTCATTT CAGACAGGTC CAAGTCTTT GAGTCTTCTG GACGGCTTCC CTTCGCCTGA
 61 GCCGTGATCA ACAAAATTAAAT ACTTCGAAAA ATTCTGCTGA TTTGGTTAAT CTTTTTCTGA
 121 CAAAAATTAC ATAAAGCTTT TTTCCAAGTT GAAAAAAAAA AAAAAAAAAA AAAAAAAAA//

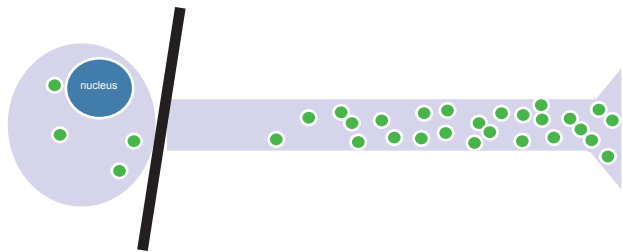


Supporting figure 2

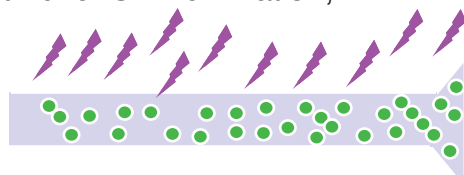
1. Microinject reporter DNA plasmid into sensory neurons;



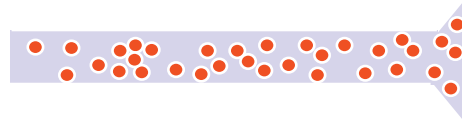
2. Remove soma after reporter expression;



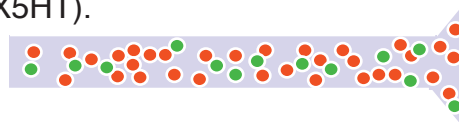
3. Photoconvert dendra from green to red with brief UV illumination;



4. Efficient photoconversion results in little dendra green signal;



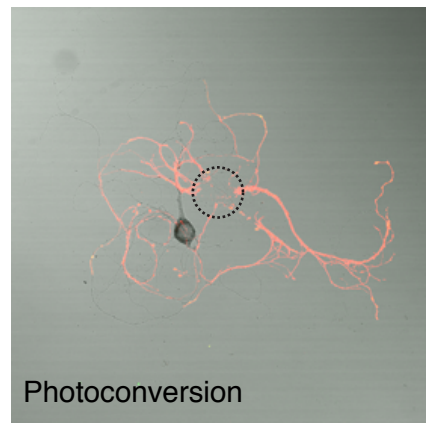
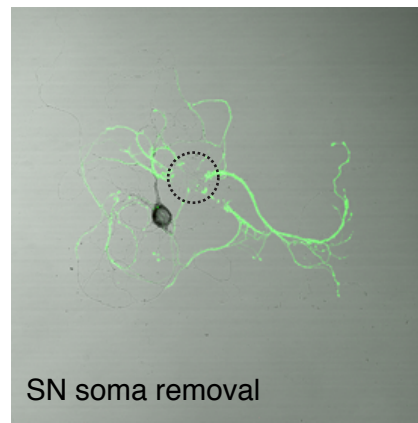
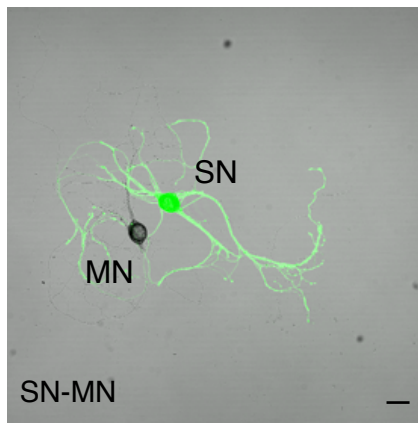
5. Detect new translation by monitoring green dendra during long-term facilitation (5X5HT).



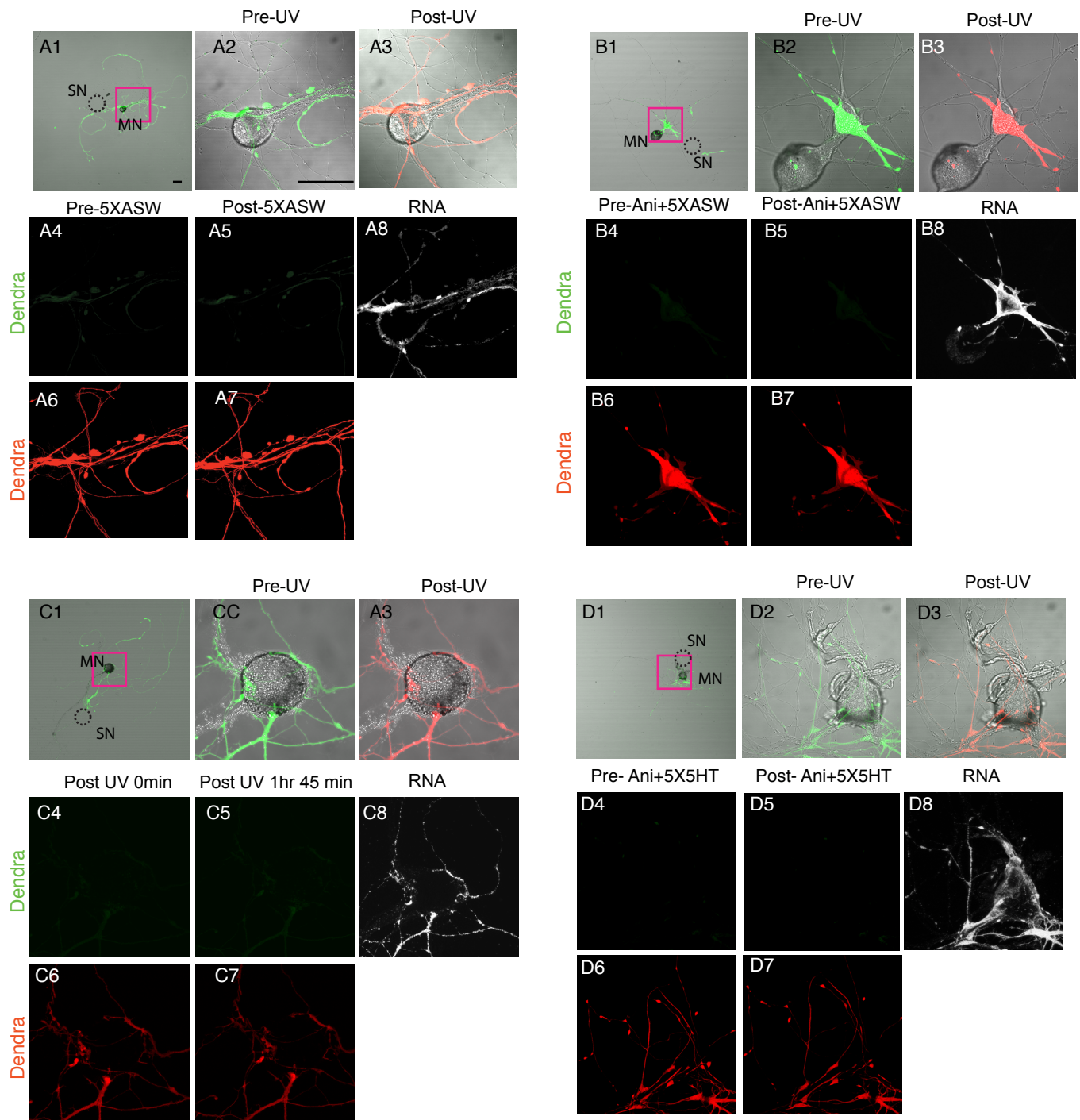
● Photoconverted dendra protein

● Newly synthesized dendra protein

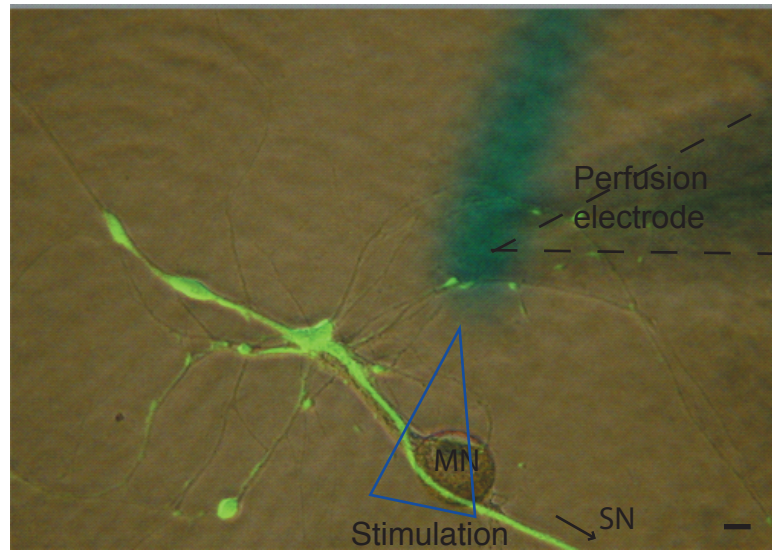
Demonstration of step 1 to 3 in neurons:



Supporting figure 3

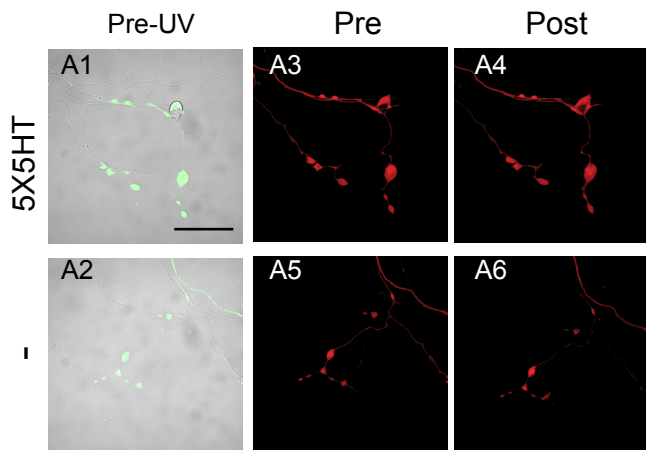


Supporting figure 4

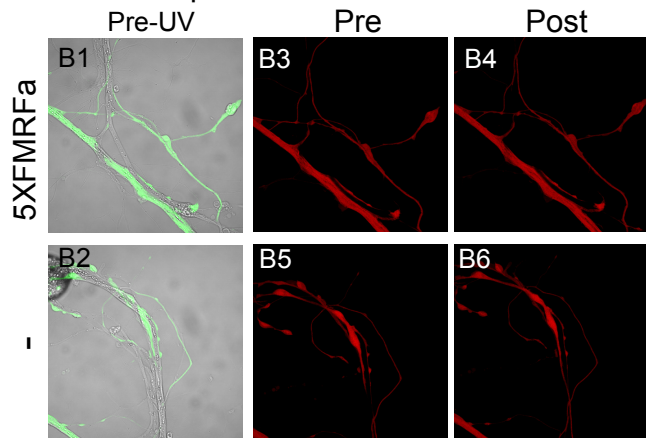


Supporting figure 5

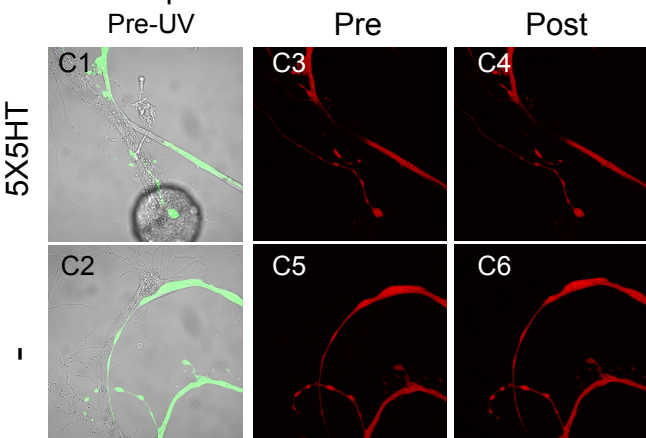
A 5'3'UTR reporter



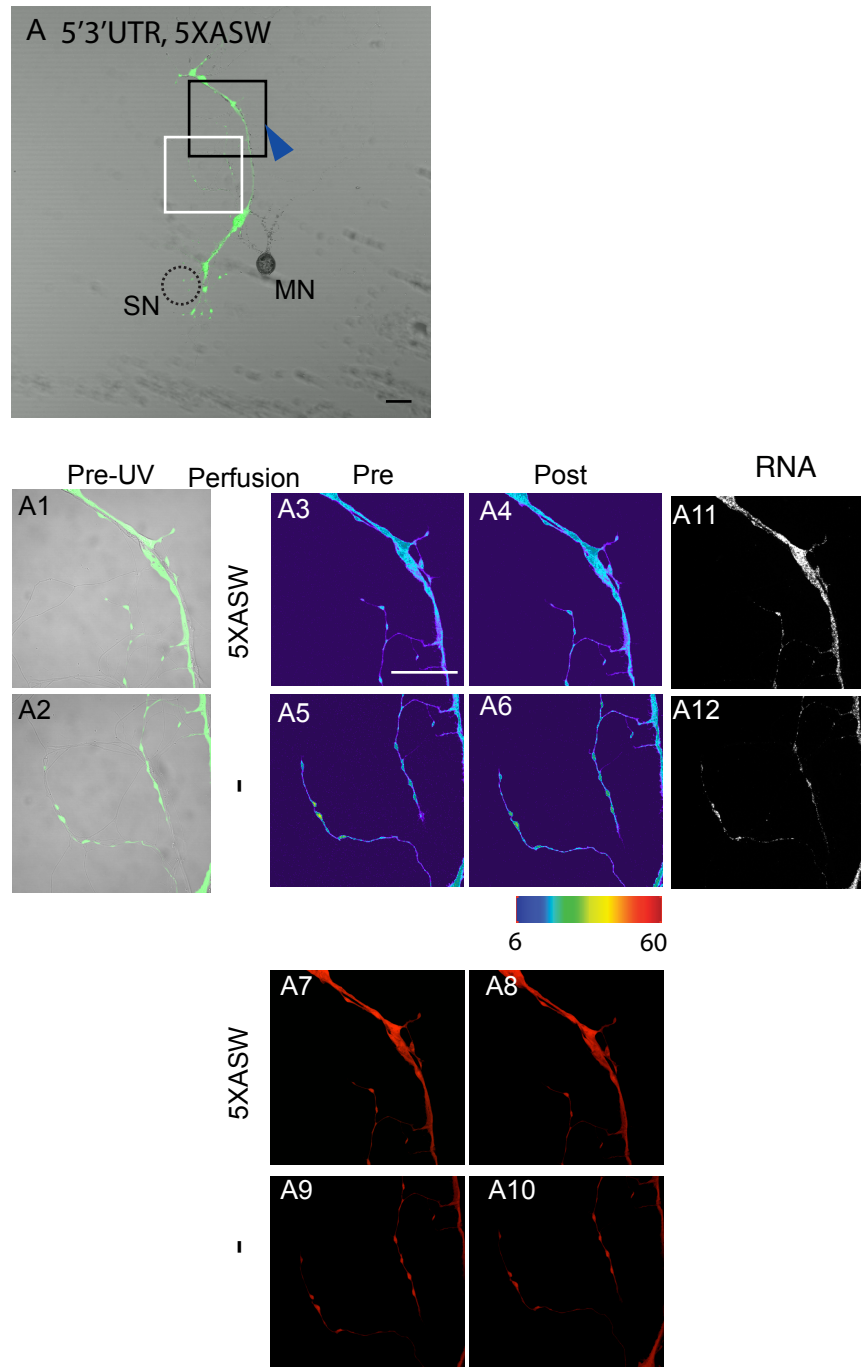
B 5'3'UTR reporter



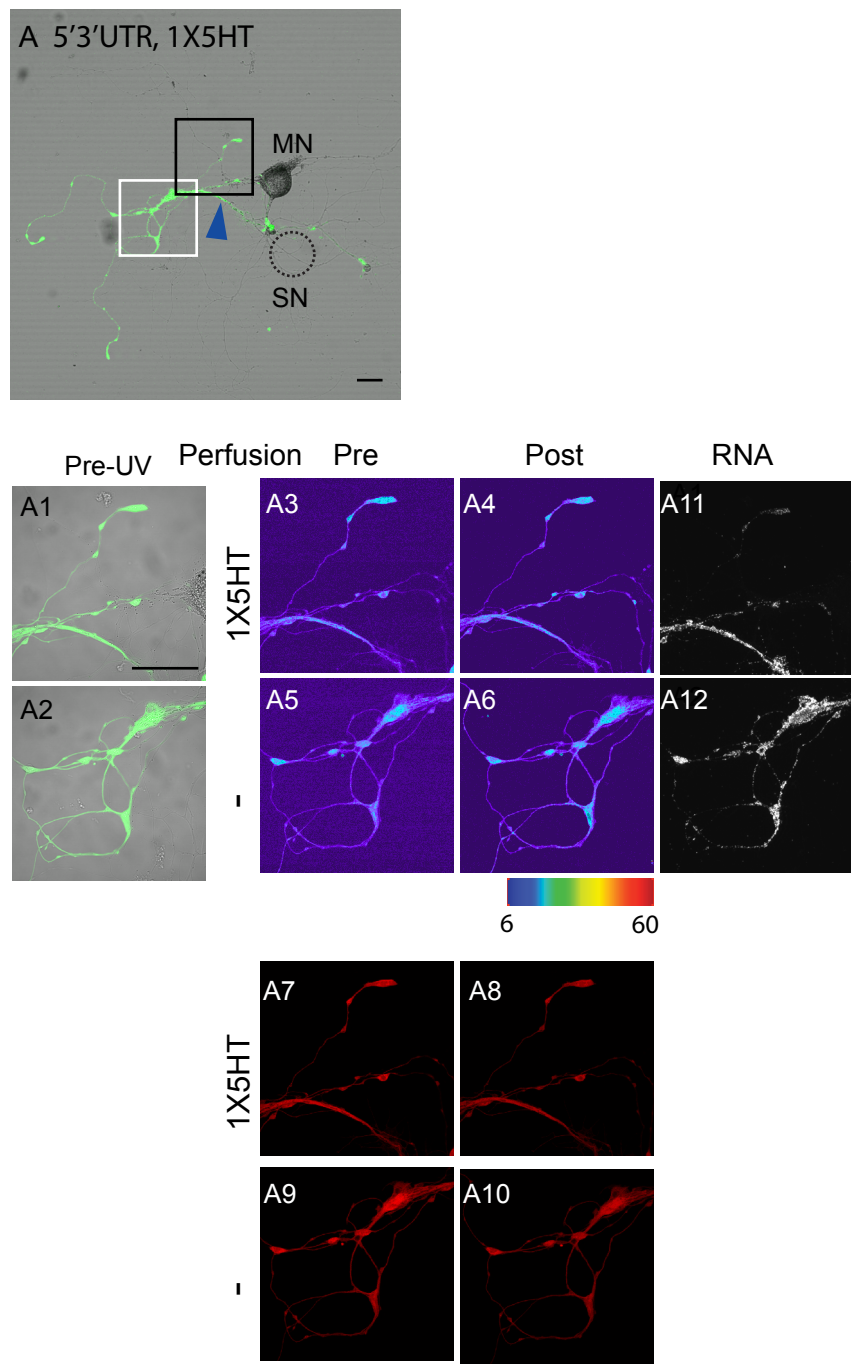
C 3'UTR reporter



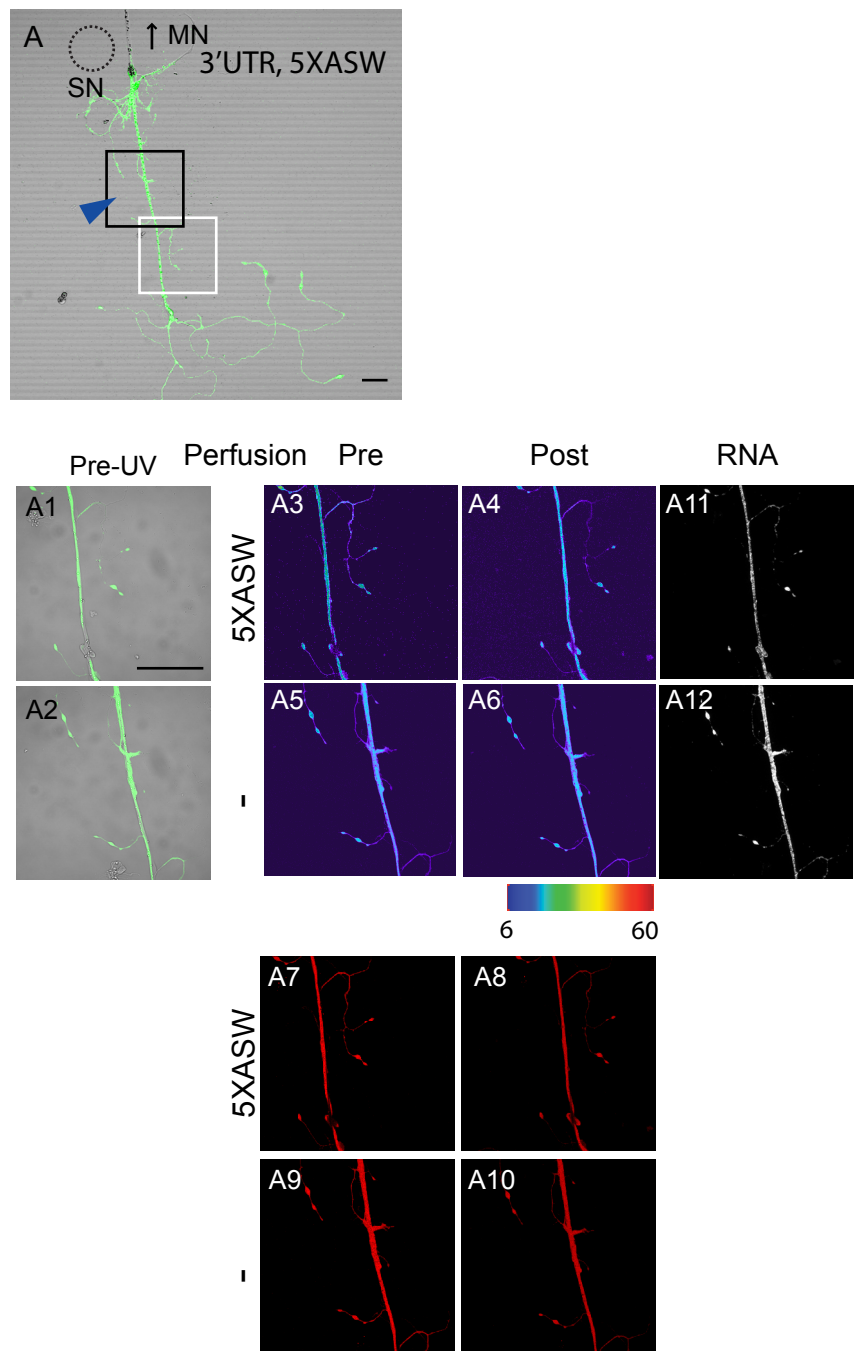
Supporting figure 6

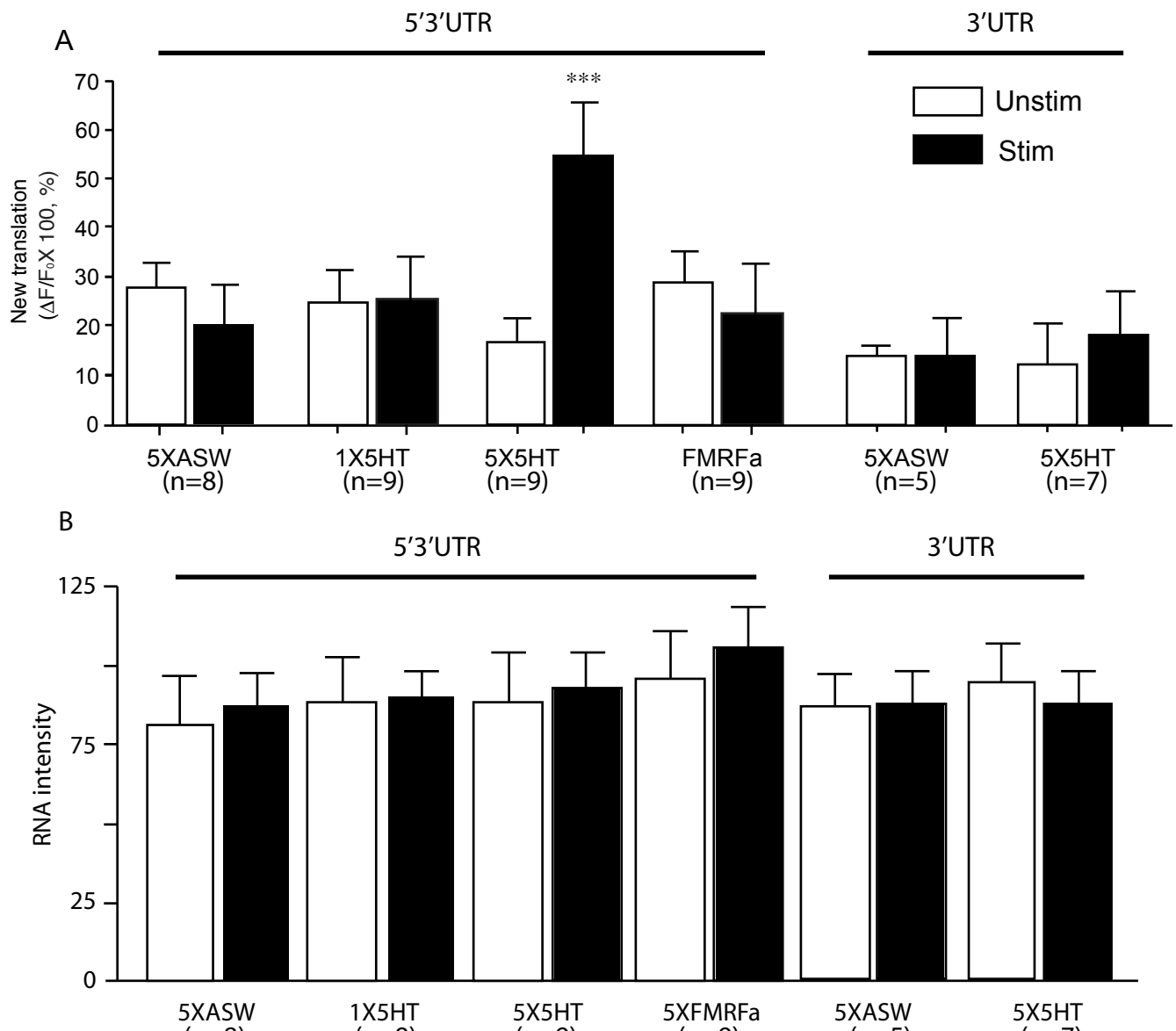


Supporting figure 7



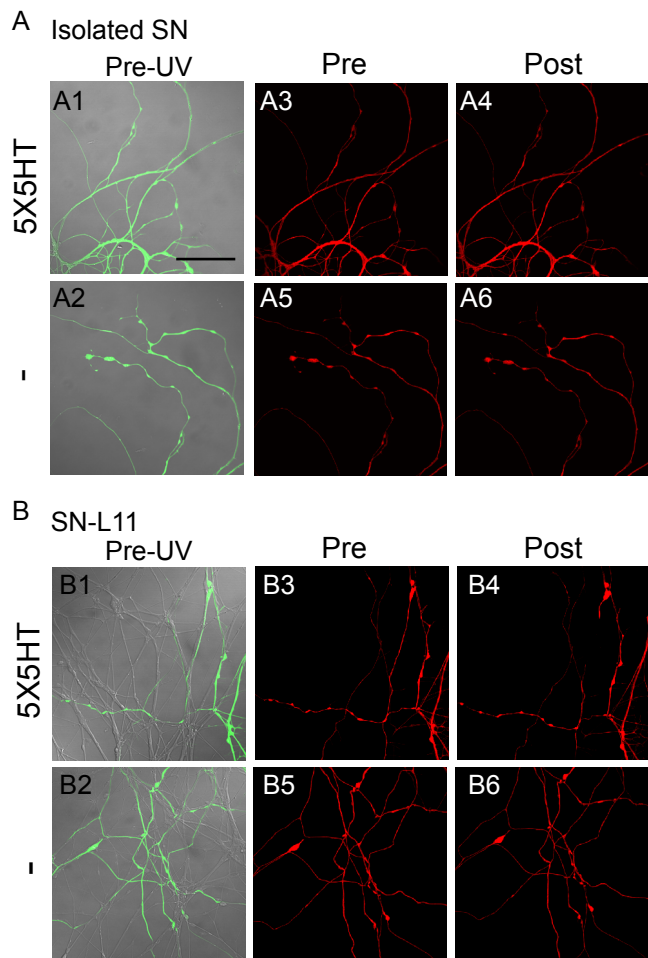
Supporting figure 8





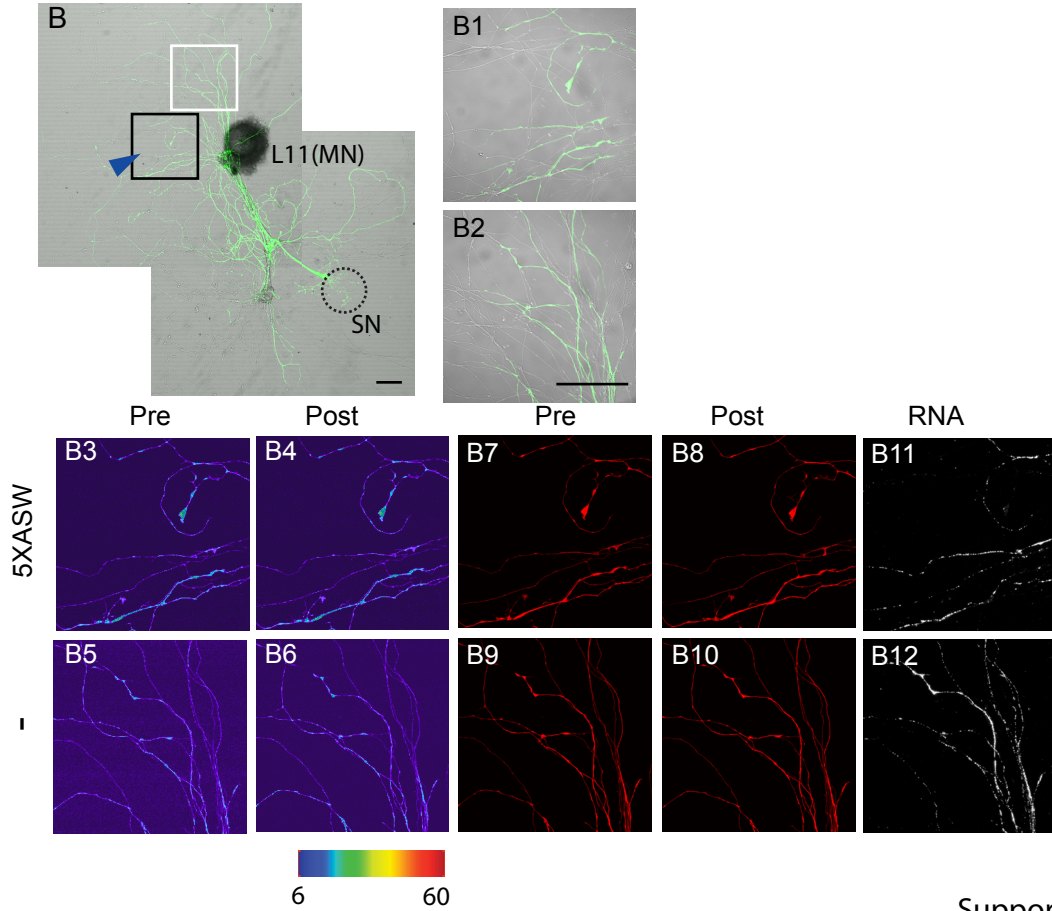
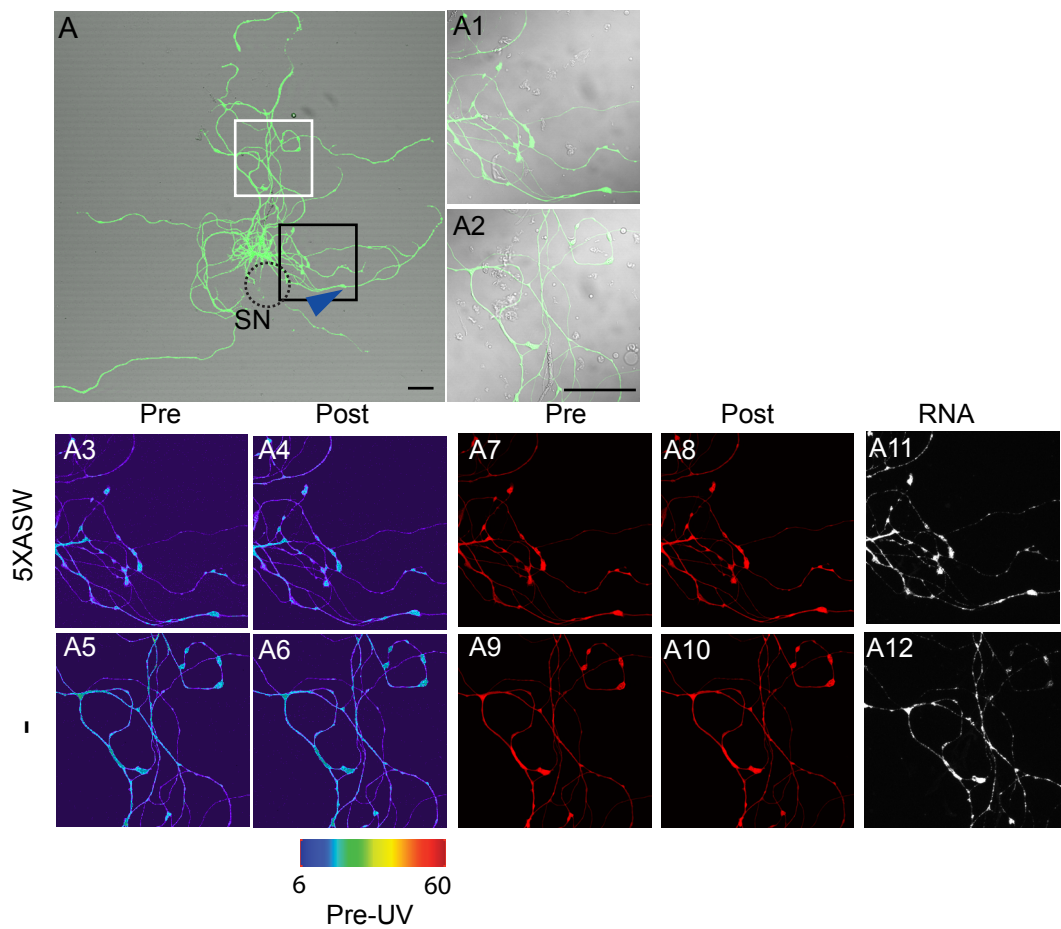
Translation at perfused and nonperfused sites measured as $\Delta F/F$

Supporting figure 10

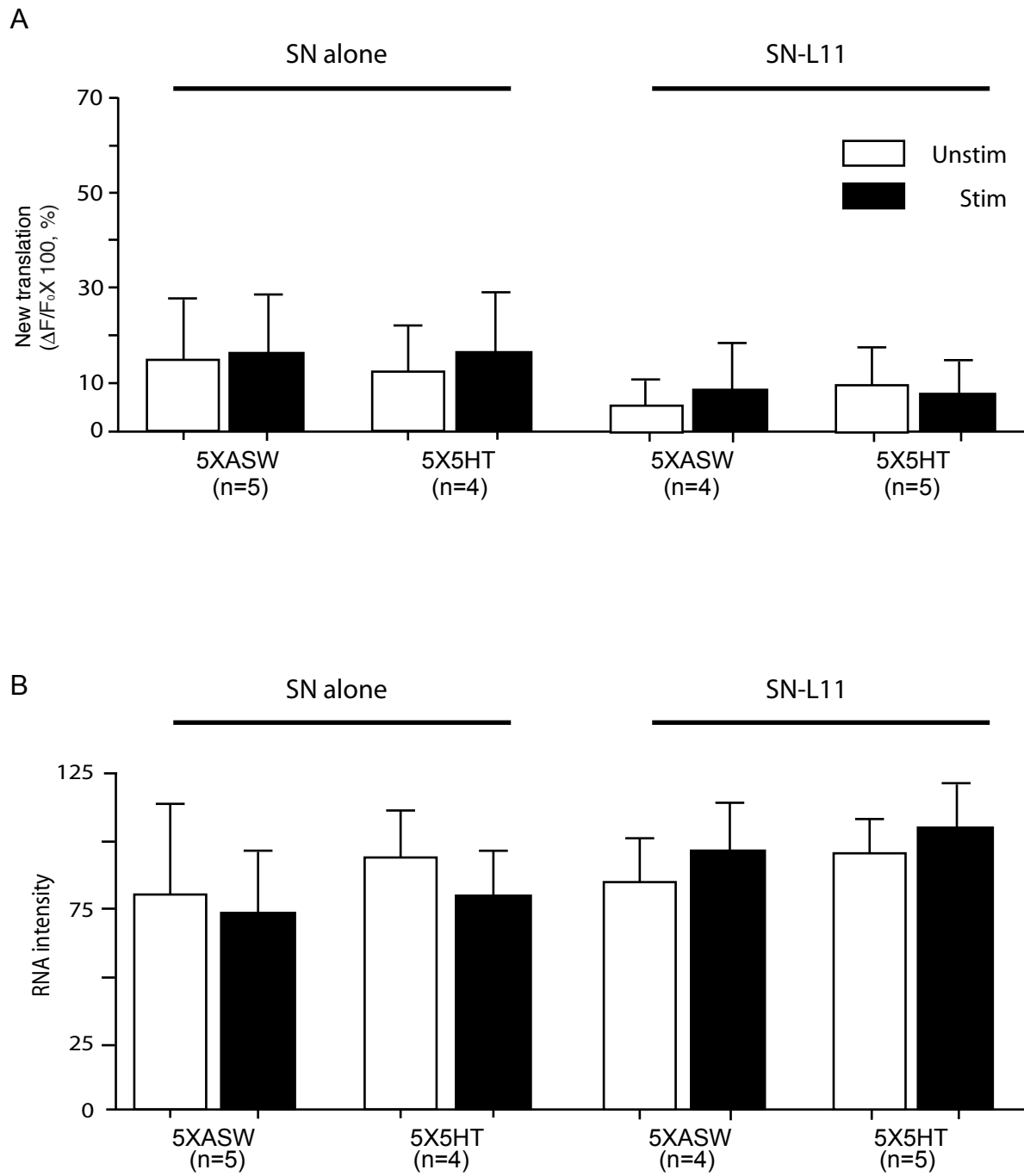


Supporting figure 11

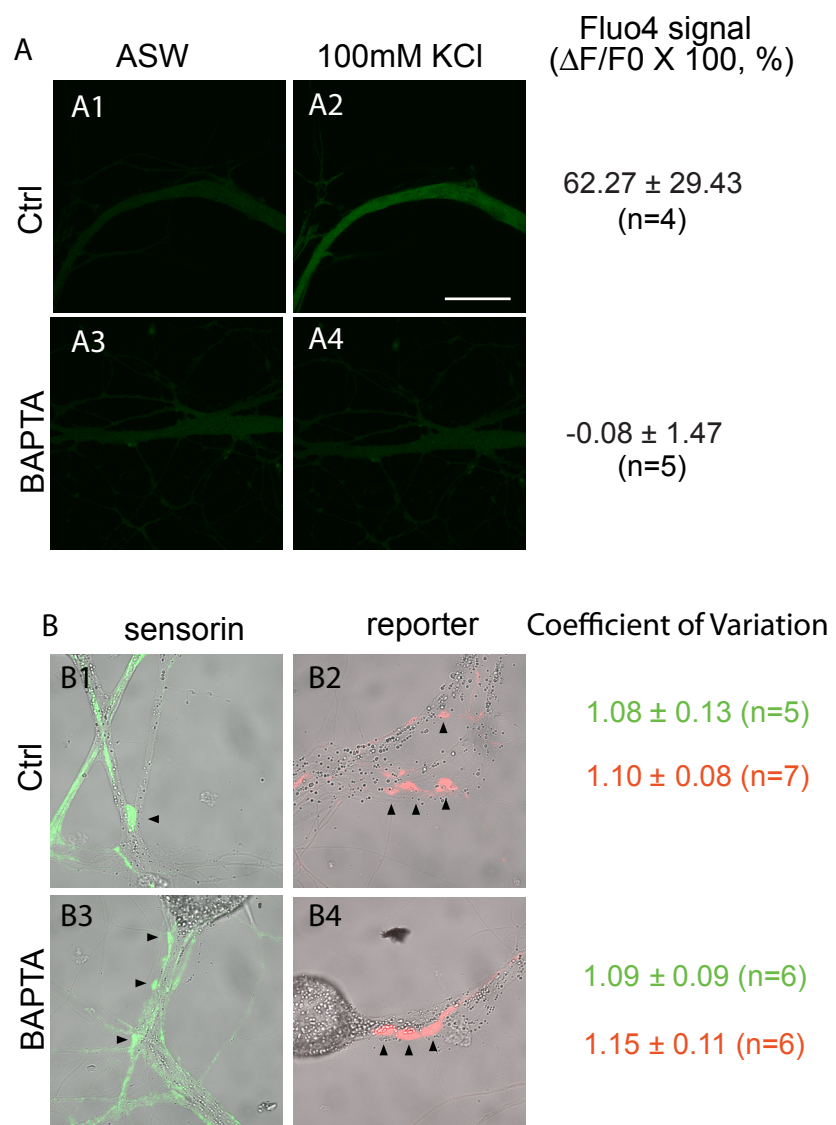
Pre-UV



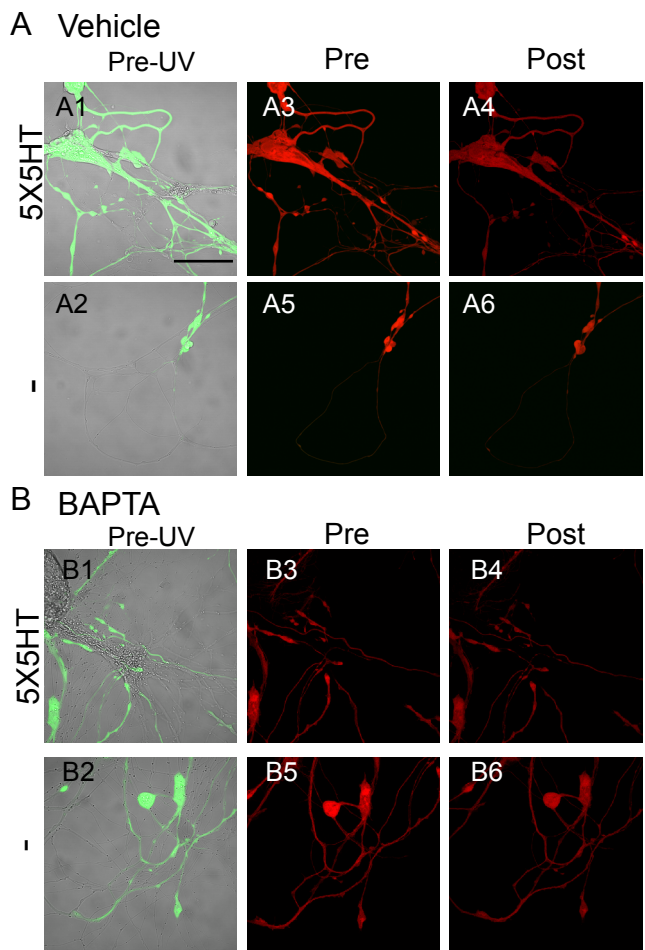
Supporting figure 12



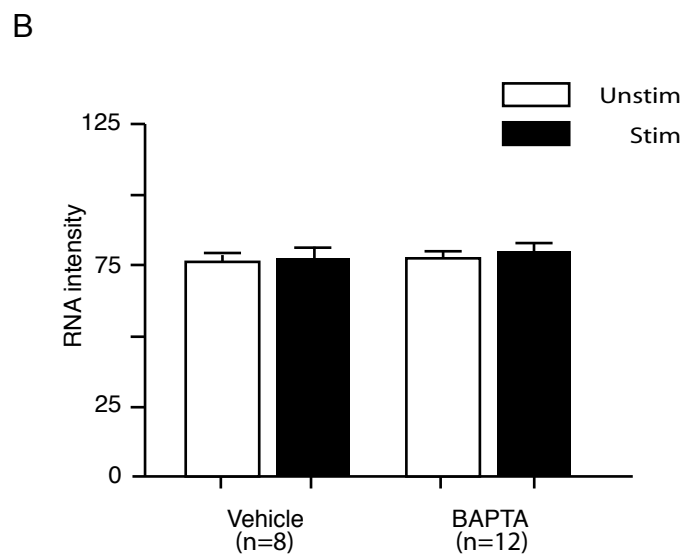
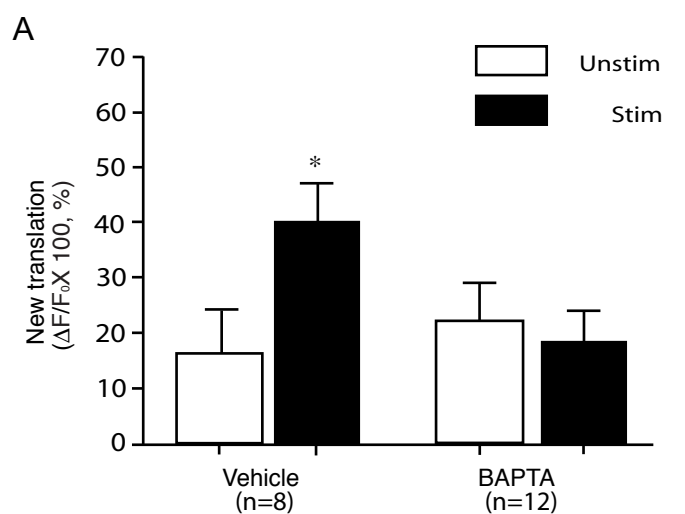
Supporting figure 13



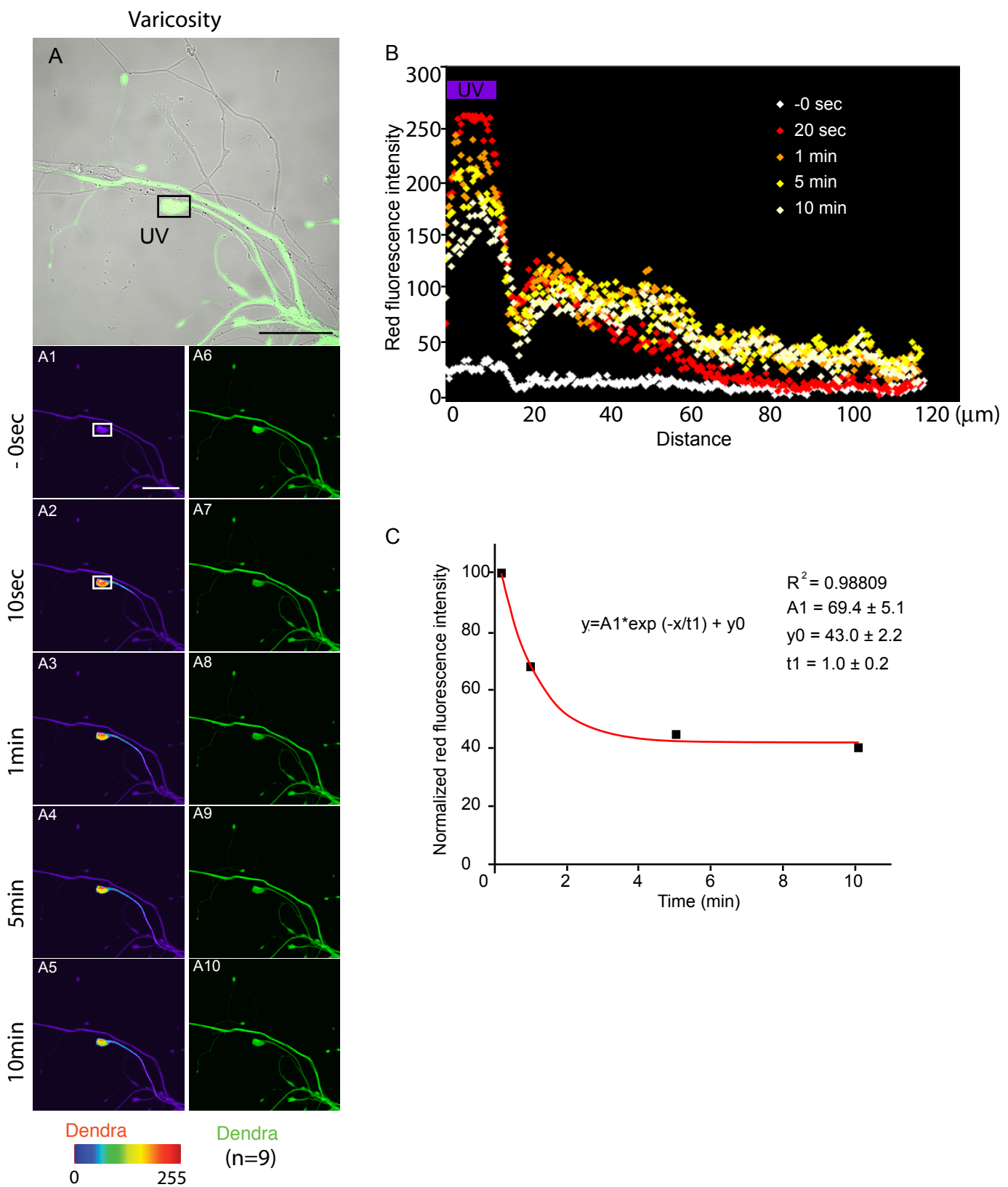
Supporting figure 14



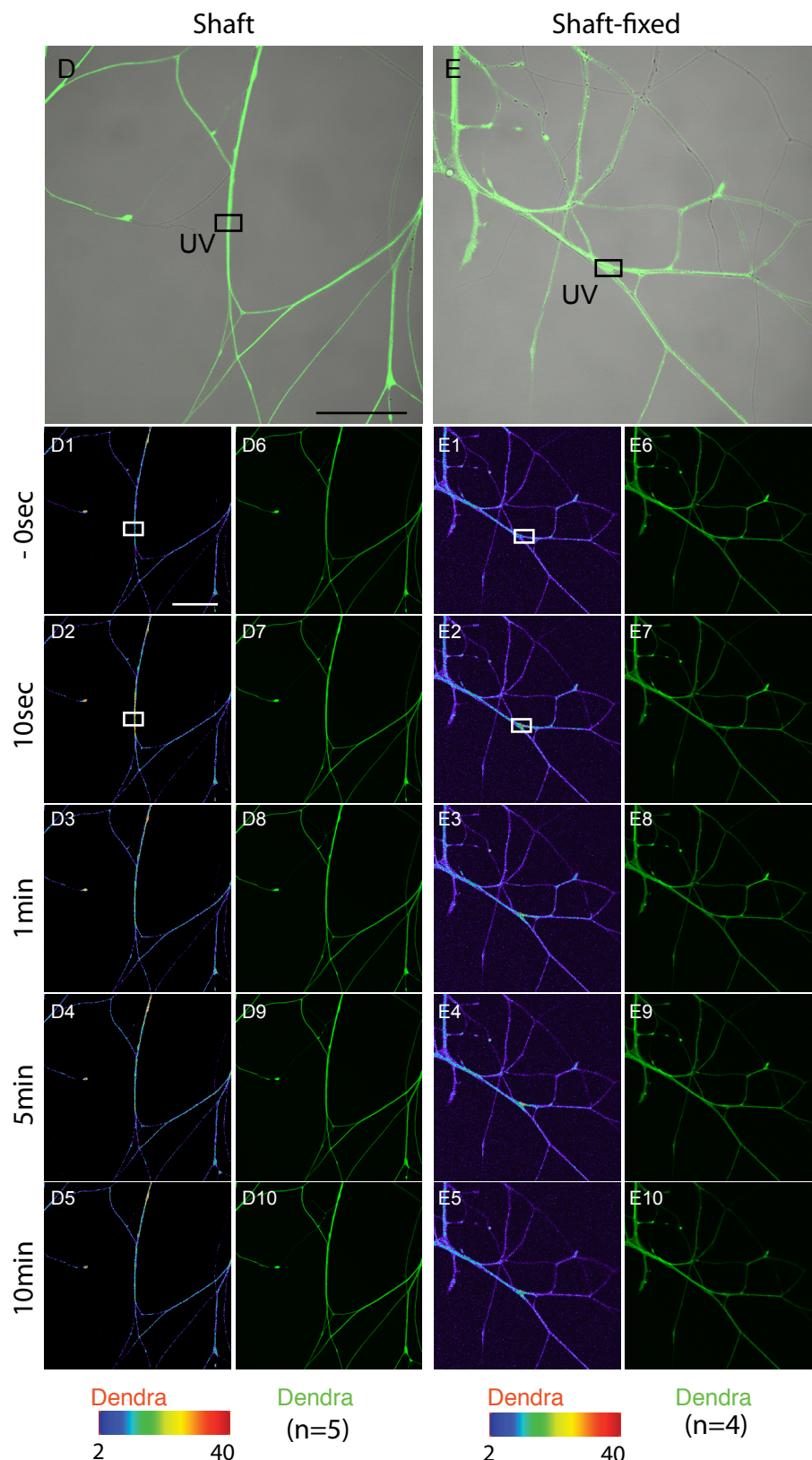
Supporting figure 15



Supporting figure 16



Supporting figure 17 A-C



Supporting figure 17 D, E